Progress In Electromagnetics Research M, Vol. 113, 173–185, 2022

A Novel Two Port MIMO Antenna Having Dual Stopped-Band Functionality and Enhanced Isolation

Muhammad K. Khan and Quanyuan Feng*

Abstract—This article introduces a unique dual-band notched Ultra Wide Band (UWB) Multiple Input Multiple Output (MIMO) antenna. The planned MIMO antenna has two identical Mushroom-shaped radiators with a combined dimension of $18 \times 34 \times 1.6\,\text{mm}^3$. Inverted L-structured stubs are joined to the antenna's ground to provide enhanced port isolation. The proposed antenna achieves improved isolation of 23 dB over 3.08–12.8 GHz bandwidth. Two novel strips are extruded in the antenna's ground and mushroom-shaped radiator to introduce a notched WiMAX band (3.37–4.30) and WLAN (5.08–5.80) GHz band. The presented antenna's peak gain is achieved from 2 to 4.8 dBi, and the antenna's radiation efficiency is attained between 78 and 90% except for (3.37–4.30) GHz and (5.08–5.80) GHz stopped bands.

1. INTRODUCTION

The improvement in advanced technology helped us to attain high data rate communication. UWB technology has numerous advantages of channel capacity and faster data rate [1]. However, UWB technology suffers from the problem of indoor environmental limited coverage and the issue of multipath fading. To solve these issues, a MIMO system is combined with UWB technology to expand coverage, boost efficiency, and give greater channel capacity [2]. Several MIMO antennas with different port isolation enhancement techniques have been introduced in the literature. In article [3], orthogonally placed circular radiating components are printed for UWB communications. The compact antenna's size is $25 \times 25\,\text{mm}^2$ with resonant frequency varying from 3.1 to 12 GHz. Different slots and slits are initiated to enhance isolation to 15 dB in the entire UWB. A quadrant-shaped antenna with band filtering abilities is designed [4]. The antenna's isolation is 18 dB with secured bandwidth of 3.06–11 GHz. Complementary split ring resonators (CSRR) and capacitive loaded loop (CLL) resonators are added for WiMAX and WLAN band-notched characteristics. In article [5], a Vivaldi antenna with dimensions of $26 \times 26\,\text{mm}^2$ is initiated for UWB applications. The antenna's working bandwidth is 2.9–11.6 GHz and achieves 16 dB port isolation. The two stopped bands are achieved by placing SRRs near the fed line. In article [6], a $40 \times 20\,\text{mm}^2$ size square-shaped antenna with working bandwidth of 3–11 GHz is discussed. Pin diodes and parasitic resonators are recommended to obtain WiMAX and WLAN band-notched characteristics.

Two stepped radiating elements are initiated to achieve the wide bandwidth of 2–13.7 GHz and 20 dB isolation [7]. The gain of the suggested antenna ranges between 1.1 and 4.3 dBi. In [8], the authors fabricated a small UWB MIMO antenna with a frequency bandwidth of 3.05–11.65 GHz. The 5G band is achieved by etching a CSRR on radiating components. A WiFi application is achieved by loading a SRR in antenna's ground. The antenna's efficiency is 58%; envelope correlation coefficient (ECC) is 0.02; and diversity gain (DG) is greater than 9.94 dB. To reduce mutual coupling, a 46 mm × 32 mm size coplanar waveguide coplanar waveguide (CPW)-fed UWB MIMO antenna is developed [9]. The working

Received 14 July 2022, Accepted 29 August 2022, Scheduled 21 September 2022
* Corresponding author: Quanyuan Feng (fengquanyuan@163.com).
The authors are with the School of Information Science and Technology, Southwest Jiaotong University, Chengdu 611756, China.

bandwidth is from 3 to 16 GHz with dual-notched band abilities. The dual bands are stopped by using step impedance resonator (SIR) to microstrip and the cup-shaped branch to the ground plate. By introducing periodic strip branches behind radiating elements, the suggested antenna's mutual coupling is decreased. An orthogonal placed circle-shaped antenna with dual stopped band abilities and 21 dB enhanced isolation is fabricated [10]. The antenna achieves the desired bandwidth of 2.36–12 GHz with 3.37–3.98 GHz and 4.71–5.51 GHz notched bands. ECC of the printed antenna is ≤ 0.04 with DG $\geq$ 9.99 dB. A fractal-shaped $36 \times 63\,\text{mm}^2$ size antenna with achieved bandwidth (3–11.1) GHz is designed [11]. The 3.5 GHz centered notched band is obtained by etching slots in the radiators. In article [12], a $25 \times 25\,\text{mm}^2$ dimension UWB antenna operating in 2.97–13.8 GHz bandwidth is fabricated. A cross-shaped un-connected ground stub is proposed to enhance isolation. The proposed antenna secures ECC ≤ 0.05 and DG $\geq$ 9.97 dB. A $40 \times 40\,\text{mm}^2$ orthogonal placed UWB MIMO antenna with a combination of CPW and microstrip fed diversity application is presented [13]. The CPW-fed antenna operates in 2.7–11 GHz, and the microstrip-fed antenna operates in 3–10.6 GHz bandwidth. The enhanced isolation is between 20 and 25 dB. The planned antenna's maximum gain is between 3 and 5 dBi, and the antenna achieves 80% radiation efficiency.

In study [14], a UWB MIMO antenna having wearable jeans substrate is introduced to increase port isolation. The $35 \times 35\,\text{mm}^2$ size antenna achieves an operating bandwidth of 1.71–12.63 GHz. An eight branches tree-shaped stub is introduced to enhance isolation further. The ECC of the presented antenna is ≤ 0.012 and DG $\geq$ 9.9 dB. A dual ports low-profile UWB MIMO antenna is introduced for switchable filtered-band abilities [15]. Pin diodes with L-shape slots are used for the reconfigurable band-notched application. A V-cut shape patch antenna is presented for the WLAN 5.4 GHz band [16]. The size of the antenna is $32 \times 56\,\text{mm}^2$ with 13 dB secured isolation. The ECC of the printed antenna is 0.0004, and it also achieves 4.3 dBi gain. In article [17], a $21 \times 27\,\text{mm}^2$ size UWB MIMO antenna is investigated for band-notched abilities. The antenna's vast working bandwidth ranges from 3 to 11 GHz and mutual coupling $\leq$ 15 dB. Four L-shaped slots are etched to achieve band-notched properties. A CPW-fed octagonal-shaped transparent antenna is presented [18]. The transparent antenna is introduced to operate in the desired 3–5 GHz frequency. The port isolation is $\leq$ 20 dB, and the ECC ranges from 0.02 to 0.45. In article [19], a simple UWB MIMO antenna having band-notched functionality is presented. A 5.8 GHz WLAN filtered band is observed by etching symmetrical slots in the partial ground. Pin diodes are initiated to control the stopped bands. The dimension of the orthogonal placed disc-shaped antenna is $45 \times 26\,\text{mm}^2$ with notched band reconfiguration properties. The port isolation is $\geq$ 20 dB. In study [20], a $35 \times 40\,\text{mm}^2$ throne-shaped MIMO antenna is introduced. The antenna operates in 2.9–11.5 GHz frequency bandwidth with dual-band rejection ability for 5.50 and 7.50 GHz bands. The dual band rejection ability is achieved by using a U-slot in the strip and an SRR on the ground plane. The 22 dB desired isolation is secured by using a cone-shaped stub with a rectangular shape slot. The simulated results are validated with the experimental results in an anechoic chamber. A $41 \times 30\,\text{mm}^2$ dimension UWB MIMO antenna with operating bandwidth (3.04 to 10.87 GHz) is proposed [21]. It is designed to achieve high isolation by etching an E-shaped slot into the radiating component and a narrow slot into the ground. CADFEKO tool is used for the simulation of the antenna. A half-hexagonal antenna having circular ring resonator (CRR) and ground stub is designed [22]. The antenna size is $20 \times 34\,\text{mm}^2$, and the working bandwidth is 3–11 GHz. A half-hexagonal stub is presented to confirm 20 dB improved isolation.

2. ANTENNA DESIGN AND INVESTIGATION

A compact MIMO antenna is printed on an easily accessible 1.6 mm thick FR4 substrate. The relative permittivity of the FR4 substrate is 4.4 with a loss tangent of 0.02. The radiating element, microstrip line, and the ground are made of copper with a thickness of 0.035 mm. The $18 \times 34\,\text{mm}^2$ mushroom-shaped antenna radiating component consists of rectangular and half-circular patches for the adjustment of lower frequencies. To enhance isolation between two ports, a pair of inverted L-shaped stubs are introduced as shown in Figure 1. To stop the interference of WiMAX and WLAN, L- and T-shaped strips are introduced in the radiator and ground, respectively. The width and length of the radiating patches are varied till the impedance bandwidth characteristics of VSWR < 2 are achieved.

Two novel strips are used to stop the WiMAX and WLAN interferences. The dimensions of the

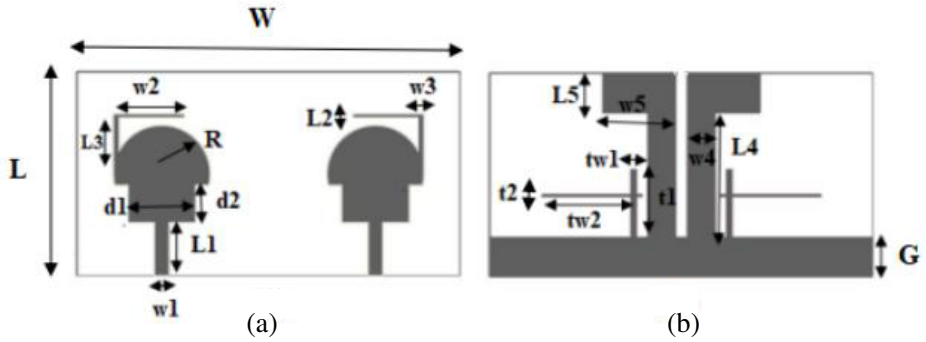

Figure 1. Views of the submitted antenna from (a) top and (b) bottom.

strip have been optimized in a way that the performance of the individual notched frequencies and the antenna's UWB performance are not affected. The band notch is determined from Equation (1) [23].

$$L = \frac{c}{4f_n\sqrt{(\varepsilon_r + 1)/2}} \tag{1}$$

The strip length is denoted by L, notched frequency by f_n, speed of light by c, and relative permittivity of the substrate by (ε_r).

After analyzing and examining the dimension of the antenna, the detailed dimensions of the suggested antenna are $W = 34$, $L = 18$, $G = 3.5$, $R1 = 4.3$, $d1 = 6$, $d2 = 3.8$, $L1 = 4.74$, $w1 = 1.3$, $L2 = 0.3$, $w2 = 6.1$, $L3 = 4.8$, $w3 = 0.5$, $L4 = 11$, $w4 = 2.5$, $L5 = 3$, $w5 = 6.5$, $t1 = 5.8$, $tw1 = 0.4$, $t2 = 0.25$, $tw2 = 9.3$.

For the UWB MIMO antenna, the most important characteristic is to obtain the entire UWB. To obtain the UWB range, a simple rectangular antenna with a microstrip fed line is designed in Figure 2(a).

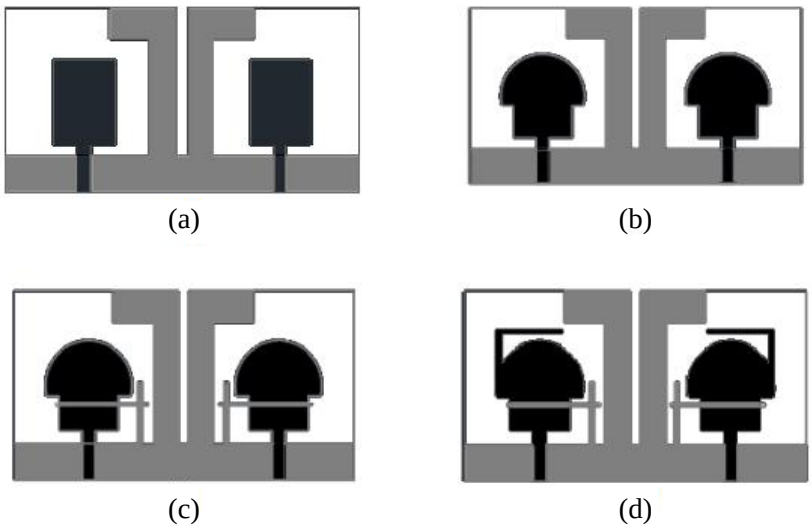

Figure 2. Plotting of the printed antenna. (a) Rectangular antenna, (b) mushroom-structured antenna, (c) mushroom-structured antenna with T-shaped strip, and (d) mushroom-structured antenna with L and T-shaped strips.

The rectangular antenna operates in 3.11–12.8 GHz bandwidth, as shown in Figure 3(a). The rectangular antenna is transformed into a mushroom-shaped antenna after adding a half circle to the rectangular radiator in Figure 2(b) to achieve UWB spectrum. The mushroom-shaped antenna works from 3.08–12.8 GHz fulfilling the criteria of the UWB range as given in Figure 3(b). However, several

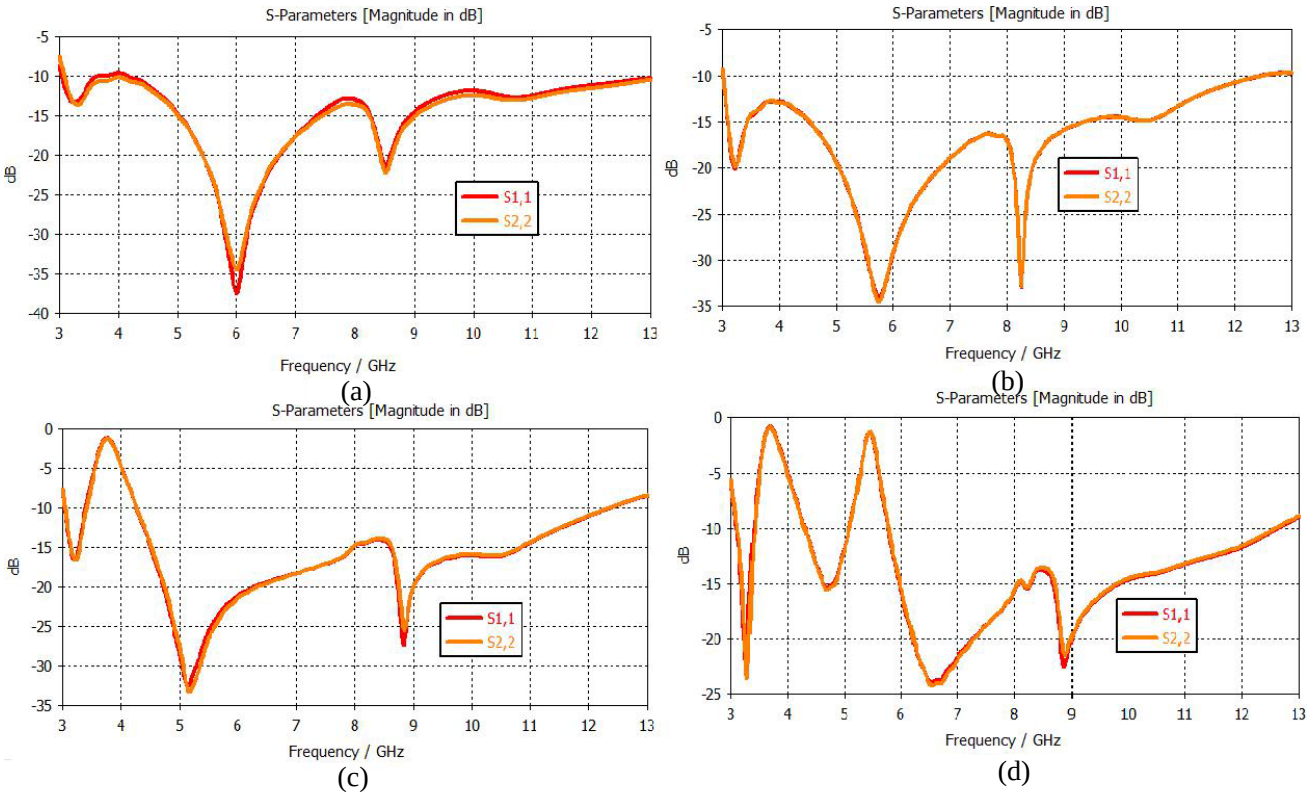

Figure 3. S_{11}/S_{22} for different antenna structures. (a) Rectangular antenna, (b) mushroom-shaped antenna, (c) mushroom-shaped antenna with T-shaped strip, and (d) proposed antenna with L and T-shaped strips.

narrowband systems cause interference in the UWB range. To remove these disturbances in the UWB range, a novel T-shaped strip is initiated in the antenna's ground to prevent the interruption of the WiMAX band (3.37–4.30) GHz. A simple L-shape strip is included in the radiating patches of the designed antenna to filter out the interference of the WLAN band (5.08–5.80) GHz.

Two inverted L-shaped stubs are included in the antenna ground as a decoupling structure to enhance isolation as clear from Figure 4. In Figure 4(a), an ordinary ground is created and tested for results. The S_{12}/S_{21} of the proposed antenna with the ordinary ground is near 12 dB, and thus further modification is needed. To enhance the isolation further, an I-shaped stub is added to the ordinary ground plane in Figure 4(b), and it is tested for results. The results with an I-shaped stub are improved from that of ordinary ground, but some modifications are needed to enhance the isolation at lower frequencies. To achieve the required improved isolation, a vertical slot is etched in the I-shaped vertical stub, another horizontal stub is added, which is further transformed into inverted L-shaped stubs in Figure 4(c). In Figure 4(d), the effect of a T-shaped strip on the performance of an inverted L-shaped stub is studied as a final step.

The S-parameters of the antenna having different decoupling structures are given in Figure 5. It is confirmed from Figure 5(a) that the results with the conventional ground are near 12 dB. After the conventional ground is modified to an I-shaped stub, the results are tested, and it is clear from Figure 5(b) that the port isolation is enhanced from that of conventional ground. To obtain the desired isolation of 23 dB, the I-shaped stub is further modified to an inverted L-shaped stub, and it is clear from Figure 3(c) that the results with inverted L-shaped stubs are far better than those with the ordinary ground and I-shaped stubs. In MIMO antennas, high isolation is always desired. Figure 5(d) confirms that the inverted L-shaped stub performance is not affected too much by the T-shaped strip.

The detailed parametric study of the proposed antenna radiators, ground, stubs, and strips is carried out in this section. The S_{11} parameter of the antenna is defined as the reflection coefficient at

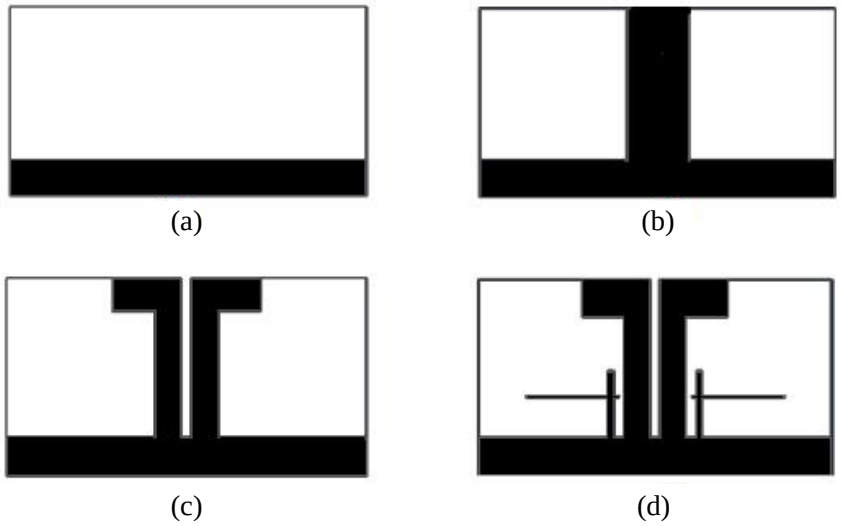

Figure 4. Transformation of decoupling geometry. (a) Ordinary ground, (b) I-shaped stub, (c) inverted L-shaped stubs, and (d) inverted L-shaped stubs with T-shaped strips.

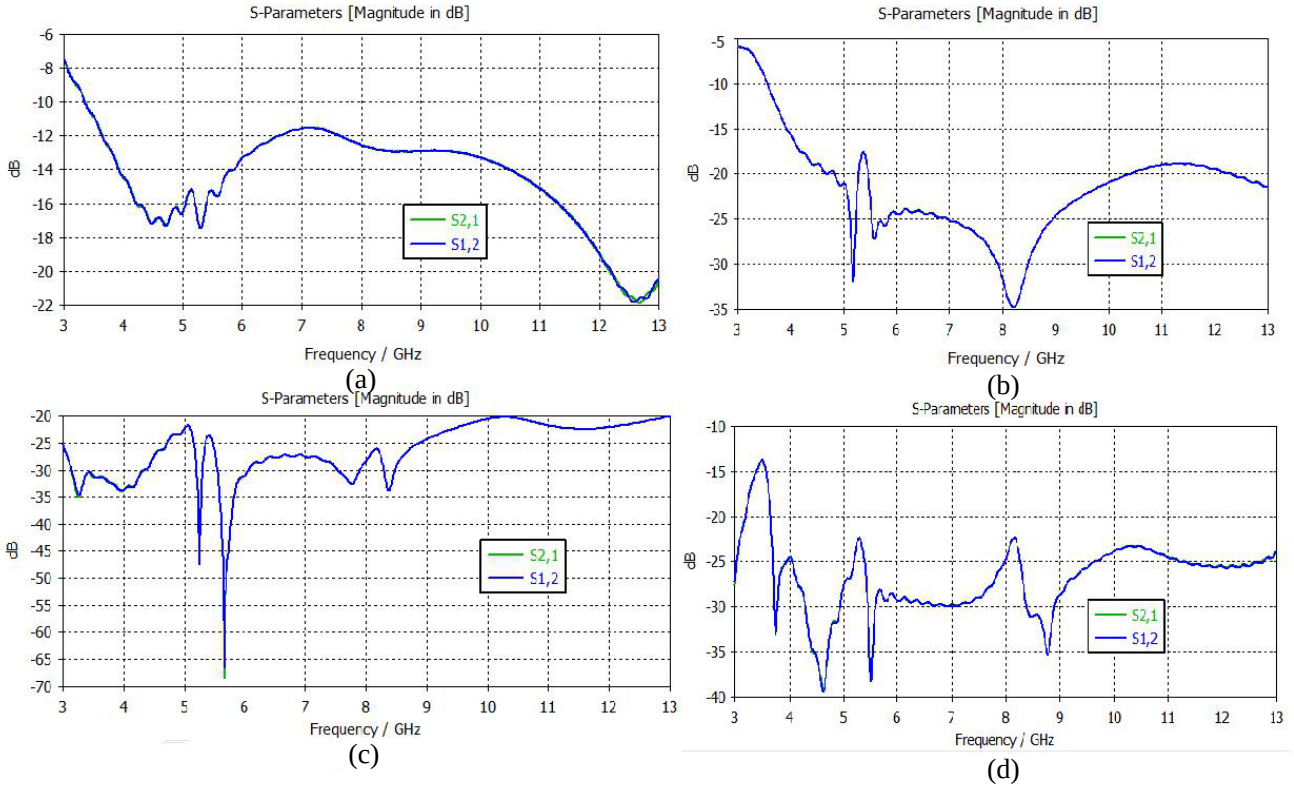

Figure 5. Analysis of S_{12}/S_{21} of various stub structures for antenna design. (a) Ordinary ground, (b) I-shaped stub, (c) inverted L-shaped stubs, and (d) inverted L-shaped stubs with T-shaped strips.

port 1, and S_{22} is the reflection coefficient at port 2. If the result of S_{11} and S_{22} is equal to zero, the antenna is virtually radiating nothing. In the first step, the rectangle ($d1$) of the mushroom-shaped radiator with different size values is examined, and its effect on the return loss is investigated. As clear from Figure 6(a), when the length of $d1$ is 6 mm, S_{11}/S_{22} is less than -16 dB in the entire UWB

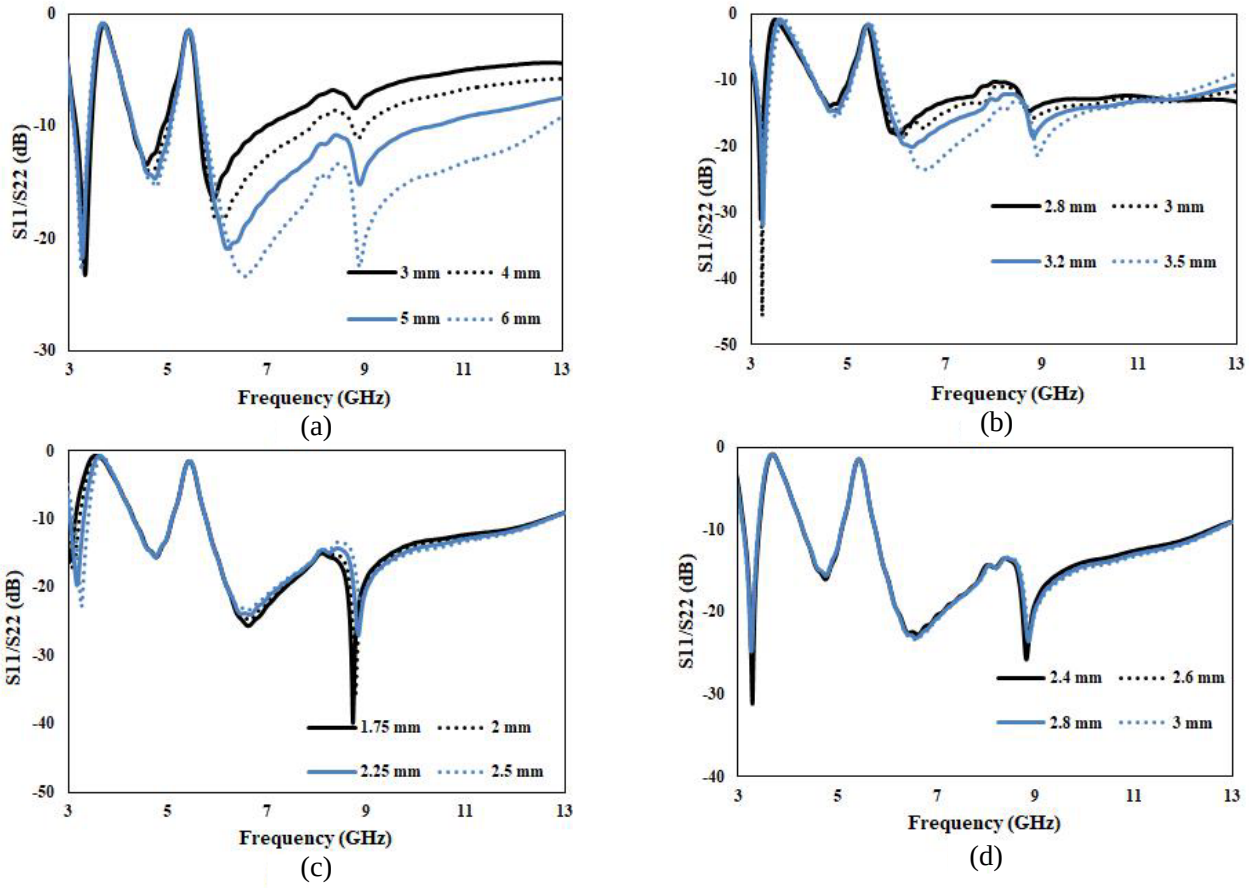

Figure 6. S-parameters results of the designed antenna. (a) Results with different sizes of rectangle $d1$, (b) the antenna's performance with ground G, (c) results for I-shaped stub $w4$, and (d) results for horizontal stub $L5$.

range with two stopped bands for WiMAX and WLAN. The effect of ground on antenna performance is examined by varying the ground size. Four different ground (G) sizes are taken. It is clear from Figure 6(b) that S_{11}/S_{22} is less than -20 dB in most of the UWB range when its size is 3.5 mm. The effect of the I-shaped stub on the antenna's performance is marginal as given in Figure 6(c). It is clear from Figure 6(c) that when the I-shaped stub size is varied to 2.5 mm, the antenna's performance gets better. The impact of the horizontal stub on antenna performance is given in Figure 6(d), and it is clear from Figure 6(d) that the result with the size of 3 mm is a good impact on the antenna's performance.

To evaluate the antenna's performance further, the effect of the L- and T-strip on the antenna's S-parameters is given in Figure 7. The antenna radiates well when S_{11} and S_{22} of the antenna are less than -10 dB. The T-strip impact on the antenna's performance is shown in Figure 7(a). The strip $t1$ with four different sizes is studied, and it is confirmed from Figure 7(a) that $t1$ with size 5.8 mm gives good results. The strip $tw2$ effect on the antenna's reflection coefficient is shown in Figure 7(b), and it confirms that the antenna gives good results with a size of 9.3 mm. To investigate the effect of the L-shaped strip, results for $L3$ and $W2$ are given in Figure 7(c) and Figure 7(d). Figure 7(c) confirms that when the size of $L3$ is 4.8 mm, its results are improved. The effect of strip $w2$ has a better result with a size of 6.1 mm as clear from Figure 7(d). After analyzing the sizes of the rectangle, ground, stubs, and strips, the detailed antenna parameters are given in millimeters.

To demonstrate the antenna's performance further the recommended antenna's current distribution is presented in Figure 8. The designed antenna's Port 1 is excited and Port 2 terminated. In the first step, the antenna's current distribution without strips is analyzed at a 3.66 GHz frequency. Figure 8(a) confirms that the strong maximum current occurs at the feed line, radiating element, and

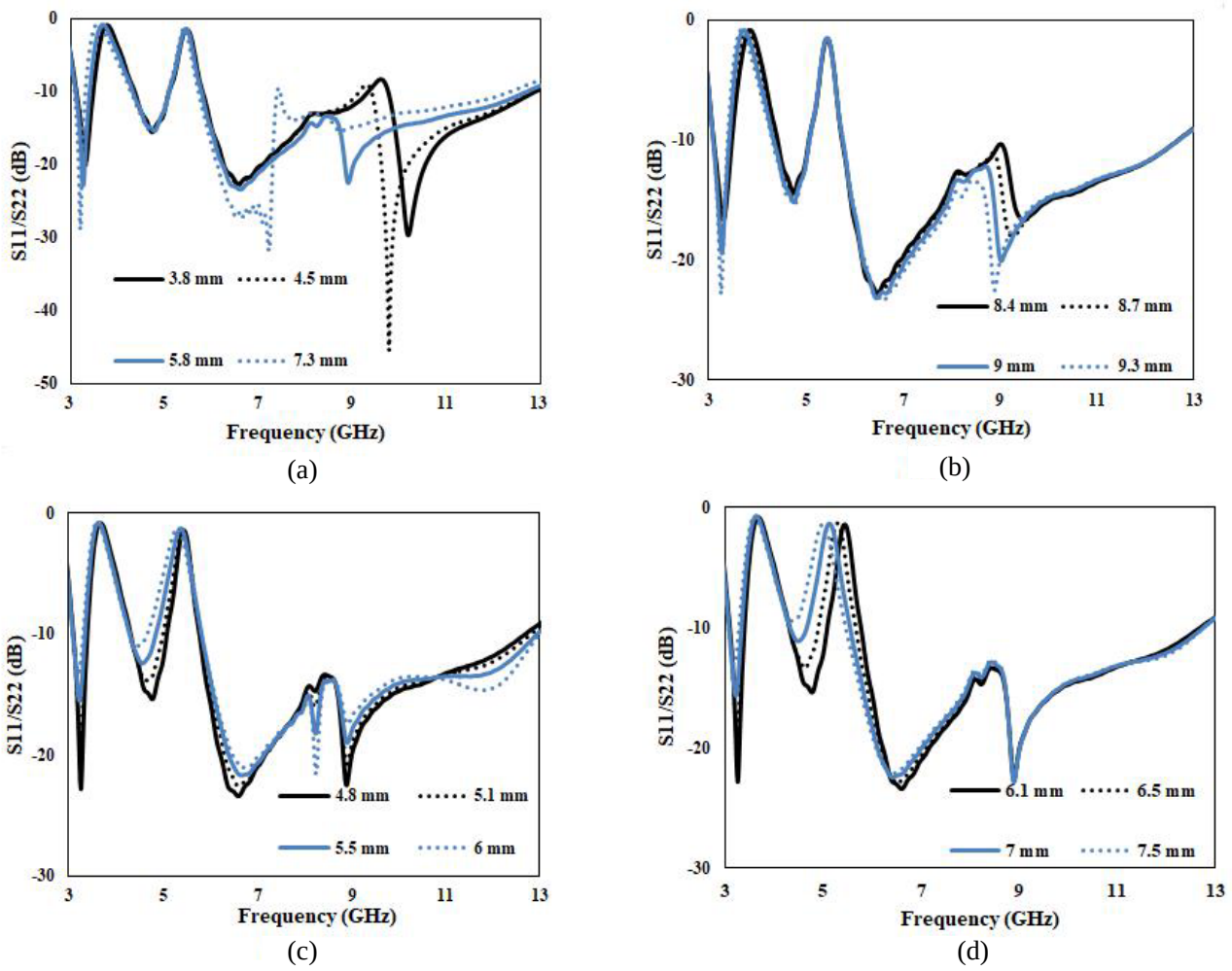

Figure 7. S_{11}/S_{22} results of the suggested antenna. (a) Results for T-strip $t1$, (b) results for T-strip $tw2$, (c) results for L-strip $L3$, and (d) results for L-strip $w2$.

decoupling stub. The current distribution is again analyzed at 3.66 GHz after adding the T- and L-shaped strips. The maximum current occurs at the T-shaped strip and right side of the inverted L-shaped stub, resulting in a deep WiMAX notched band as shown in Figure 8(b). In Figure 8(c), the current distribution of the presented antenna without notched band properties is examined at 5.45 GHz frequency, and Figure 8(c) shows that maximum current occurs at the feed line, radiating element, and inverted L-shaped decoupling stub. After attaching the strips to the ground and radiator, the current distribution is again analyzed at 5.45 GHz as confirmed in Figure 8(d), that maximum current occurs at the L-shaped strip resulting in a deep WLAN notched band.

3. RESULTS AND DISCUSSION

The printed MIMO antenna contains two identical mushroom-shaped radiators, two inverted L-shaped stubs, a T-shaped strip, a ground plane, and an L-shaped strip. CST Studio is used for the simulation of the proposed design. To validate and analyze the simulated results further, the antenna is fabricated, and the results are measured. The top and bottom views of the antenna are displayed in Figure 9.

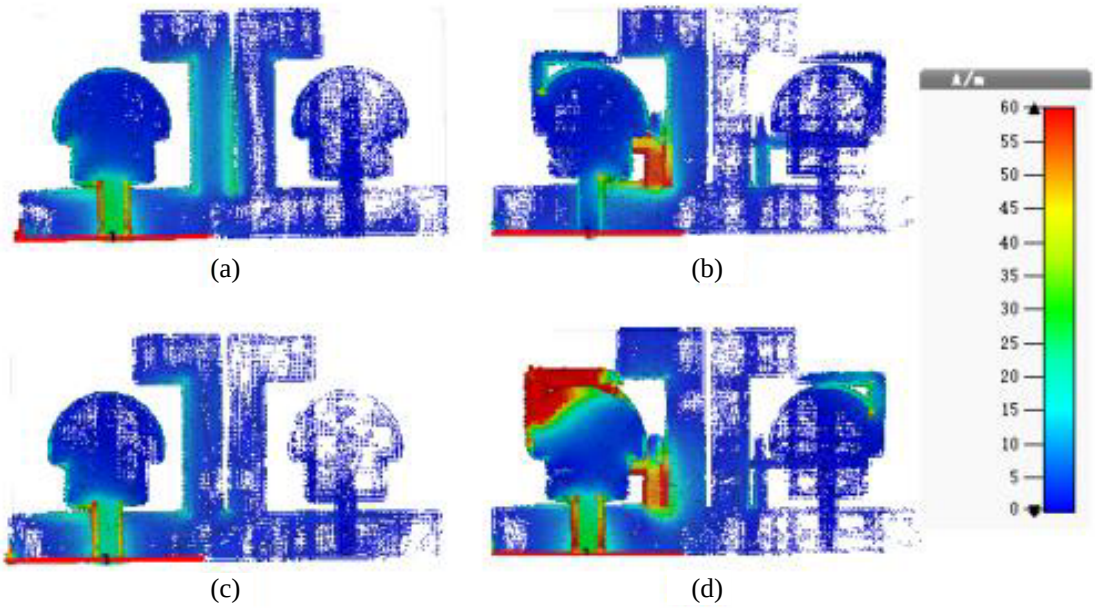

Figure 8. The UWB MIMO antenna's current distribution (a) with inverted L-shaped stub at 3.66 GHz, (b) with stub and strips at 3.66 GHz, (c) with inverted L-shaped stub at 5.45 GHz, and (d) with stub and strips at 5.45 GHz.

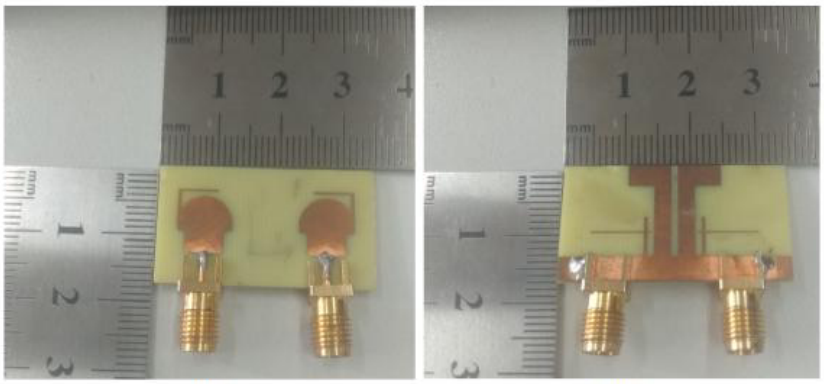

Figure 9. (a) Top and (b) bottom view of the fabricated antenna.

3.1. Reflection Coefficient

The achieved S_{11} is -10 dB in 3.08–12.80 GHz bandwidth except for the notched bands 3.37–4.30 GHz and 5.08–5.80 GHz as shown in Figure 10. The notched band WiMAX (3.37–4.30) GHz is attained by attaching a T-shaped strip to the antenna ground plane. Another L-shaped strip is connected to the radiating patch to obtain the (5.08–5.80) GHz WLAN band. Two Inverted L-shaped stubs are used to enhance isolation. The simulated and measured $|S_{12}|/|S_{21}|$ are below 23 dB as clear from Figure 10. The simulated and measured S_{11} and S_{22} of the proposed antenna are less than -15 dB in the entire UWB range with dual stopped bands for WiMAX and WLAN. It is clear from Figure 10 that the antenna radiates properly in the entire UWB spectrum. The simulated and measured S_{12} and S_{21} are below 23 dB which confirms that the power transferred to both ports from one another is very minimum.

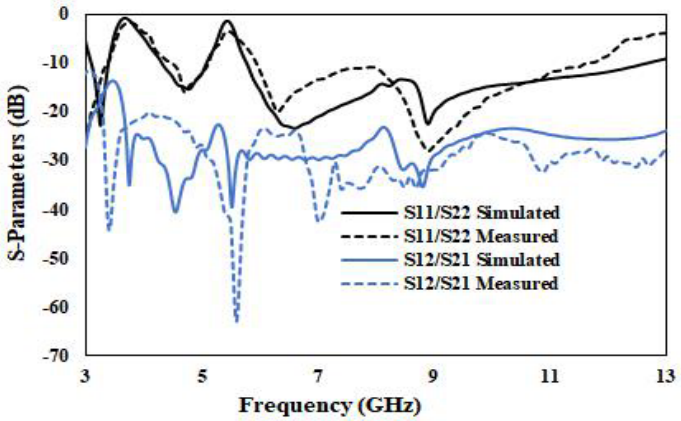

Figure 10. *S*-parameters of the designed antenna.

3.2. Radiation Patterns, Radiation Efficiency and Peak Gain

To evaluate the MIMO antenna performance further the radiation patterns of the proposed antenna are examined. The simulated and measured radiation patterns at the *E*- and *H*-planes of the proposed MIMO antenna are illustrated in Figure 11. The radiation pattern of the monopole antenna is omnidirectional and radiates equal power in all directions perpendicular to the antenna. The simulated and measured radiation patterns of the designed antenna are studied at 4.6 GHz and 6 GHz. It is clear from Figure 11 that the resonance frequencies are stable, and the antenna's radiation pattern at both frequencies is omnidirectional.

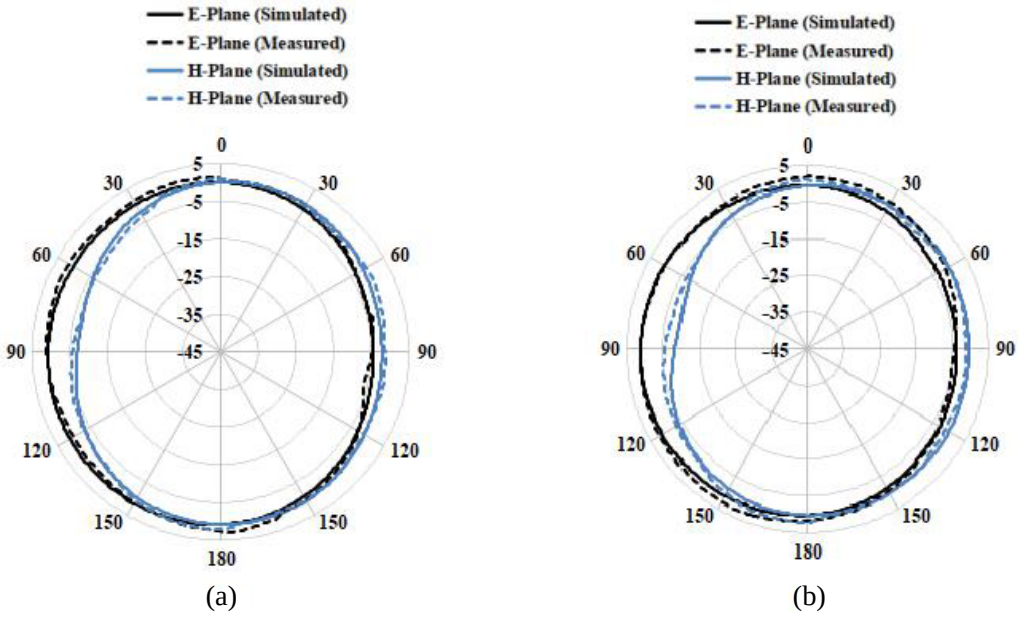

Figure 11. The presented MIMO antenna's radiation patterns. (a) 4.6 GHz and (b) 6 GHz.

The presented antenna's peak gain is from 2 to 4.8 dBi in the entire UWB except for the notched bands. The gain at WiMAX notched band is −3.5 dBi and −2 dBi at WLAN band. The antenna's radiation efficiency is from 78 to 90% except for the (3.37–4.30) GHz and (5.08–5.80) GHz stopped bands as shown in Figure 12.

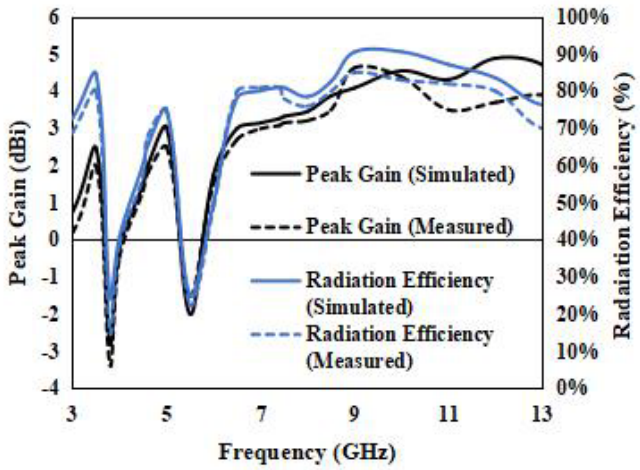

Figure 12. Radiation efficiency and peak gain of the planned antenna.

3.3. Diversity Performances of the Presented Antenna

A diversity performance evaluation is performed to further investigate the proposed antenna accuracy. The ideal value for the ECC is zero, but an experimental limit of 0.5 is allowable. ECC and the DG of the MIMO antenna are calculated using the following equations [24].

$$\mathrm{ECC} = \frac{\left|S_{11}^{*}S_{12} + S_{21}^{*}S_{22}\right|^{2}}{\left(1 - |S_{11}|^{2} - |S_{21}|^{2}\right)\left(1 - |S_{22}|^{2} - |S_{12}|^{2}\right)} \tag{2}$$

$$\mathrm{DG} = 10\sqrt{1 - (\mathrm{ECC})^{2}}. \tag{3}$$

The calculated ECC using S-parameters is less than 0.001, and the diversity gain is > 9.99 dB as shown in Figure 13. The ECC increases to 0.06 at 3.66 GHz and 0.015 at 5.45 GHz notched bands. The DG of the proposed antenna decreases to 9.7 dB at 3.66 GHz and 9.99 dB at 5.45 GHz as expected for notched bands as clear from Figure 13. A detailed comparison of the planned antenna is given in Table 1.

A compact mushroom-shaped antenna with two simple strips is suggested in this study. The presented antenna contains two identical mushroom shape radiators, two inverted L-shaped stubs, T- and L-shaped strips. As confirmed in Table 1, the proposed antenna has a miniaturized size of

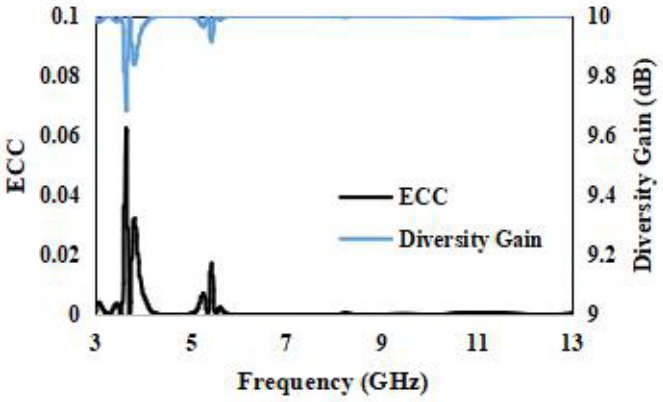

Figure 13. ECC and diversity gain of the designed antenna.

Table 1. Analyzing previous work and comparing the fabricated antenna.

Refs.	Size (mm^2)	Bandwidth (GHz)	Band notches (GHz)	Isolation (dB)	DG (dB)	ECC	Radiation efficiency (%)	Major findings
[3]	25×25	3.1–12	5.6–6.5	< 15	9.64	<0.06	—	Achieved 3.1–12 GHz bandwidth with 6.1 GHz stopped band.
[4]	24×26	3.06–11	3.5–4, 5.1–5.85	< 18	—	0.18	> 90	Achieved 3.06–11 GHz bandwidth with dual stopped bands for WiMAX and LTE band 43.
[5]	26×26	2.9–11.6	5.3–5.8, 7.85–8.55	< 16	—	< 0.02	—	Achieved entire UWB band with dual stopped band characteristics and enhanced isolation of 16 dB.
[6]	40×20	3–11	3.4–4.2, 5–6.2	< 15	—	< 0.3	80	Achieved entire UWB band with dual stopped band characteristics for WiMAX and WLAN.
[7]	33×48	2–13.7	—	> 20	9.85	0.15	—	Achieved a vast bandwidth of 2–13.7 GHz with enhanced isolation of 20 dB.
[8]	40×30	3.05–11.65	3–4.4, 5.5–6.5	15	9.94	0.02	58	The authors have achieved the entire UWB band with dual stopped band properties.
[10]	50×50	2.36–12	3.37–3.98, 4.71–5.51	< 21	9.99	< 0.04	—	The authors have achieved the entire UWB band with dual stopped band properties for WiMAX and WLAN.
[11]	36×63	3–11.1	3.3–3.7	≤ 22	—	0.1	—	The authors have achieved the entire UWB band with notched band property for 3.5 GHz band.
[12]	25×25	2.97–13.8	—	< 15	9.97	< 0.05	—	The authors have achieved the entire UWB band with enhanced isolation of 15 dB.
[20]	35×40	2.9–11.5	5.1–5.9, 7.2–7.8	22 (except 8.2–10.4 GHz)	—	< 0.035	> 73	Achieved whole UWB band with dual stopped band characteristics.
This work	18×34	3.08–12.80	3.37–4.30, 5.08–5.80	< 23	9.99	< 0.001	78–90	Achieved 3.08–12.80 GHz bandwidth with dual stopped band characteristics and enhanced isolation of 23 dB.

$18 \times 34\,mm^2$. The antenna achieves the entire UWB with dual stopped band properties. The antenna has enhanced port isolation of 23 dB. The antenna attained a high radiation efficiency of 78 to 90%. The ECC and DG results of the proposed antenna are also in appropriate limits.

4. CONCLUSION

In this article, a MIMO antenna with dual notched band properties is proposed. A novel T-shaped strip is extruded from the ground to obtain a notched WiMAX band (3.37–4.30) GHz and an L-shaped strip from the radiator to stop (5.08–5.80) GHz WLAN band. Two inverted L-shaped stubs are added to the ground plane to enhance isolation to 23 dB. The proposed antenna achieves a peak gain of 2–4.8 dBi with attained radiation efficiency of 78–90%. The antenna has good diversity performance with ECC less than 0.001 and DG greater than 9.99 dB. After evaluating the presented antenna in terms of gain, efficiency, ECC, DG, and enhanced insolation, these recommended antenna parameters suggest that it is a nice choice for UWB communication systems.

ACKNOWLEDGMENT

This research is supported by the Key Project of the National Natural Science Foundation of China under Grants 61831017, 62090012, 62031016, and the Sichuan Provincial Science and Technology Important Projects under Grants 2019YFG0498, 2020YFG0282, 2020YFG0452, and 2020YFG0028.

REFERENCES

1. Porcino, D. and W. Hirt, "Ultra-wideband radio technology: Potential and challenges ahead," *IEEE Communications Magazine*, Vol. 41, No. 7, 66–74, 2003.
2. Zhang, Z., X. Wang, K. Long, A. V. Vasilakos, and L. Hanzo, "Large-scale MIMO-based wireless backhaul in 5G networks," *IEEE Wireless Communications*, Vol. 22, No. 5, 58–66, 2015.
3. Liang, C., R. Su, P. Gao, and P. Wang, "Compact printed MIMO antenna with 6.1 GHz notched band for ultra-wideband applications," *Progress In Electromagnetics Research Letters*, Vol. 76, 77–83, 2018.
4. Biswal, S. P. and S. Das, "A compact printed ultra-wideband multiple-input multiple-output prototype with band-notch ability for WiMAX, LTEband43, and WLAN systems," *International Journal of RF and Microwave Computer-Aided Engineering*, Vol. 29, No. 6, e21673, 2019.
5. Li, Z., C. Yin, and X. Zhu, "Compact UWB MIMO Vivaldi antenna with dual band-notched characteristics," *IEEE Access*, Vol. 7, 38696–38701, 2019.
6. Mathur, R. and S. Dwari, "Compact planar reconfigurable UWB-MIMO antenna with on demand worldwide interoperability for microwave access wireless local area network rejection," *IET Microwaves, Antennas & Propagation*, Vol. 13, No. 10, 1684–1689, 2019.
7. Altaf, A., A. Iqbal, A. Smida, J. Smida, A. A. Althuwayb, S. H. Kiani, M. Alibakhshikenari, F. Falcone, and E. Limiti, "Isolation improvement in UWB-MIMO antenna system using slotted stub," *Electronics*, Vol. 9, No. 10, 1582, 2020.
8. El Omari El Bakali, H., A. Zakriti, A. Farkhsi, A. Dkiouak, and M. E. Ouahabi, "Design and realization of dual band notch UWB MIMO antenna in 5G and Wi-Fi 6E by using hybrid technique," *Progress In Electromagnetics Research C*, Vol. 116, 1–12, 2021.
9. Zhang, J., L. Wang, and W. Zhang, "A novel dual band-notched CPW-fed UWB MIMO antenna with mutual coupling reduction characteristics," *Progress In Electromagnetics Research Letters*, Vol. 90, 21–28, 2020.
10. Zhou, J.-Y., Y. Wang, J.-M. Xu, and C. Du, "A CPW-fed UWB-MIMO antenna with high isolation and dual band-notched characteristic," *Progress In Electromagnetics Research M*, Vol. 102, 27–37, 2021.
11. Bhattacharya, A., B. Roy, S. K. Chowdhury, and A. K. Bhattacharjee, "Computational and experimental analysis of a low-profile, isolation-enhanced, band-notch UWB-MIMO antenna," *Journal of Computational Electronics*, Vol. 18, No. 2, 680–688, 2019.
12. Singh, H. V. and S. Tripathi, "Compact UWB MIMO antenna with cross-shaped unconnected ground stub using characteristic mode analysis," *Microwave and Optical Technology Letters*, Vol. 61, 1874–1881, 2019.

13. Kumar, R. and N. Pazare, "A printed semi-circular disc UWB MIMO/diversity antenna with cross shape slot stub," *Wireless Personal Communications*, Vol. 91, 277–291, 2016.
14. Dey, A. B., U. Bhatt, and W. Arif, "Design of a compact wearable ultrawideband MIMO antenna with improved port isolation," *Turkish Journal of Electrical Engineering & Computer Sciences*, Vol. 29, 897–912, 2021.
15. Quddus, A., R. Saleem, S. Arain, S. R. Hassan, and M. F. Shafique, "Electronically reconfigurable WLAN band-notched MIMO antenna for ultra-wideband applications," *ACES Journal*, Vol. 36, No. 8, 1108–1111, 2021.
16. Kulkarni, S. and A. Kunte, "Design of V-cut patch MIMO antenna for the 5.4 GHz band," *Wireless Personal Communications*, Vol. 121, 3233–3242, 2021.
17. Wu, L., X. Cao, and B. Yang, "Design and analysis of a compact UWB-MIMO antenna with four notched bands," *Progress In Electromagnetics Research M*, Vol. 108, 127–137, 2022.
18. Lopez-Marcos, F., R. Torrealba-Melendez, M. A. Vasquez-Agustin, J. M. Munoz-Pacheco, E. I. Tamariz-Flores, and M. Lopez-Lopez, "A MIMO transparent antenna for FR1-5G communications," *Wireless Personal Communications*, Vol. 123, 3645–3660, 2022.
19. Medkour, H., S. Lakrit, S. Das, B. T. P. Madhav, and K. VasuBabu, "A compact printed UWB MIMO antenna with electronically reconfigurable WLAN band-notched characteristics," *Journal of Circuits, Systems and Computers*, Vol. 31, No. 3, 2250045, 2022.
20. Agarwal, M., J. K. Dhanoa, and M. K. Khandelwal, "Construction of compact two-port throne-shaped antenna with dual stopbands and high isolation for ultrawideband multiple-input multiple-output wireless communication systems," *International Journal of Communication Systems*, Vol. 35, No. 11, e5195, 2022.
21. Bhanumathi, V. and G. Sivaranjani, "High isolation MIMO antenna using semi-circle patch for UWB applications," *Progress In Electromagnetics Research C*, Vol. 92, 31–40, 2019.
22. Mathur, R. and S. Dwari, "A compact UWB-MIMO with dual grounded CRR for isolation improvement," *International Journal of RF and Microwave Computer-Aided Engineering*, Vol. 29, No. 1, e21500, 2019.
23. Pannu, P. and D. K. Sharma, "Miniaturize four-port UWB-MIMO antenna with tri-notched band characteristics," *Microwave and Optical Technology Letters*, Vol. 63, No. 5, 1489–1498, 2021.
24. Khan, M. I., M. I. Khattak, S. U. Rahman, A. B. Qazi, A. A. Telba, and A. Sebak, "Design and investigation of modern UWB-MIMO antenna with optimized isolation," *Micromachines*, Vol. 11, No. 4, 432, 2020.